

 Open access • Journal Article • DOI:10.1063/1.1409964

Short wave phase shifts by large free surface solitary waves: Experiments and models — [Source link](#)

[Katell Guizien](#), [Eric Barthélemy](#)

Published on: 13 Nov 2001 - [Physics of Fluids](#) (American Institute of Physics)

Topics: [Cnoidal wave](#), [Wave propagation](#), [Surface wave](#), [Stokes wave](#) and [Dispersion \(water waves\)](#)

Related papers:

- [Characteristics of solitary waves in four-wave interactions](#)
- [Long wavelength solitary waves in Hertzian chains](#)
- [Long-wavelength solitary waves in Hertzian chains and their properties in different nonlinearity regimes](#)
- [Experiments on strong interactions between solitary waves](#)
- [Solitary Wave Interactions with Continuous Waves](#)

Share this paper:    

View more about this paper here: <https://typeset.io/papers/short-wave-phase-shifts-by-large-free-surface-solitary-waves-qpy8jobo48>



HAL
open science

Short wave phase shifts by large free surface solitary waves. Experiments and models

Katell Guizien, Eric Barthélemy

► **To cite this version:**

Katell Guizien, Eric Barthélemy. Short wave phase shifts by large free surface solitary waves. Experiments and models. *Physics of Fluids*, American Institute of Physics, 2001, 13 (12), pp.3624-3635. 10.1063/1.1409964 . hal-00182831

HAL Id: hal-00182831

<https://hal.archives-ouvertes.fr/hal-00182831>

Submitted on 5 Feb 2020

HAL is a multi-disciplinary open access archive for the deposit and dissemination of scientific research documents, whether they are published or not. The documents may come from teaching and research institutions in France or abroad, or from public or private research centers.

L'archive ouverte pluridisciplinaire **HAL**, est destinée au dépôt et à la diffusion de documents scientifiques de niveau recherche, publiés ou non, émanant des établissements d'enseignement et de recherche français ou étrangers, des laboratoires publics ou privés.



Distributed under a Creative Commons Attribution| 4.0 International License

Short wave phase shifts by large free surface solitary waves: Experiments and models

Katell Guizien^{a)} and Eric Barthélemy

Laboratoire des Écoulements Géophysiques et Industriels, BP 53, 38041 Grenoble Cedex 9, France

(Received 2 May 2000; accepted 17 July 2001)

In this paper, we compare experiments on short gravity wave phase shifting by surface solitary waves to a Wentzel–Kramers–Brillouin–Jeffreys (WKBJ) refraction theory. Both weak interactions (head-on interaction) and strong interactions (overtaking interaction) are examined. We derive a dispersion relation and wave action conservation relation which are similar to the ones obtained for short waves refraction on slowly varying media. The model requires an exact solitary wave solution. To this end, a steady wave solution is numerically computed using the algorithm devised by Byatt-Smith [Proc. R. Soc. London, Ser. A **315**, 405 (1970)]. However, two other solitary wave solutions are incorporated in the model, namely the classical Korteweg and De Vries (KdV) [Phil. Mag. **39**, 422 (1895)] solution (weakly nonlinear/small amplitude solitary wave) and the Rayleigh [Phil. Mag. **1**, 257 (1876)] solution (strongly nonlinear/large amplitude solitary wave). Measurements of the short wave phase shift show better agreement with the theoretical predictions based on the Byatt-Smith numerical solution and the Rayleigh solution rather than the Korteweg and De Vries one for large amplitude solitary waves. Theoretical phase shifts predictions based on Rayleigh and Byatt-Smith numerical solutions agree with the experiments for $A/h_0 \leq 0.5$. A new heuristic formula for the phase shift allowing for large amplitude solitary waves is proposed as a limiting case when the short wave wave number increases. © 2001 American Institute of Physics. [DOI: 10.1063/1.1409964]

I. INTRODUCTION

In the present paper we analyze how short surface waves are modulated by free surface solitary waves. This approach may be considered as a model of a more complex interaction problem, namely nonlinear internal wave–surface wave interaction. The latter is of importance for ocean remote sensing applications. Indeed, on synthetic aperture radar (SAR) images of the ocean surface, signatures of long internal waves are due to Bragg wave modulations. From a theoretical point of view free surface solitary wave and short wave interactions is a challenging problem. Indeed standard theories for short waves do not encompass long nonlinear waves and vice versa. As a first cut one may consider two linear waves one of which is very long compared to the other. This is the approach initiated by Longuet-Higgins and Stewart.¹ They analyzed the change of the form of short surface waves riding on longer ones within the framework of linearized theory for finite depths. Interaction terms are derived from the second order of Stokes' theory, which requires the assumption of small steepness for both long and short waves. They show that the short wave has a shorter wave length and increased amplitude at the long wave's crest. This Doppler effect is interpreted as the work done by the long wave against the radiation stress of the short one. In the same paper, the authors suggest to generalize the wave action con-

servation and the dispersion relation valid for surface waves refracted by a steady current to the case of surface waves riding upon a much longer wave (Sec. IV). This implies to introduce an effective gravity resulting from the vertical accelerations of the long wave. Longuet-Higgins and Stewart¹ then show that this latter approach yields the same result as their calculations within the second-order Stokes theory as long as the vertical accelerations of the longer wave is negligible, like in shallow water (Sec. V). In a companion paper, Longuet-Higgins and Stewart² made a further step forward. They analyzed the change in amplitude of a short surface wave on a steady nonuniform current. Under the slowly spatially varying current assumption they derive the laws ruling wave amplitude, namely wave action conservation, and wave length modulations.

The linear behavior of the long wave was relaxed by Garrett³ and later, Bretherton and Garrett⁴ who generalized the results obtained by Longuet-Higgins and Stewart.² In a very general setting, using the averaged Lagrangian formulation, they show that the wave action conservation is a very general result for short linear wave of small steepness as long as they propagate on a spatially and temporally slowly varying basic state. As just mentioned, the flow characteristics of the basic state do not need to be linear and effective gravity is introduced accounting for vertical accelerations in the underlying basic state. This is highlighted by Longuet-Higgins.⁵ He applied wave action conservation to show that when the long wave is steep, up to the Stokes wave maximum steepness of 0.4432, the steepness of the short wave riding on it undergoes much more enhancement

^{a)}Present address: Observatoire d'Océanologie Biologique, BP 44, 66650 Banyuls-sur-Mer, France. Telephone: +33 4 76 82 51 17; Fax: +33 4 76 82 50 01. Electronic mail: guizien@hmg.inpg.fr

than would be predicted by the second-order of Stokes' linear theory developed in his 1960 paper. Longuet-Higgins also underlined the need for a very accurate description of the long wave, which he did through a particularly efficient algorithm.

The paper of Bretherton and Garrett⁴ is an encouragement to make alternative choices on the basic state. Naciri and Mei⁶ derived analytically the solution for a short wave riding on a long wave given by the explicit formula for Gerstner's rotational wave. They qualitatively reproduce Longuet-Higgins' numerical results, and show that instabilities can appear for sufficiently large short wave steepness compared to the long to short wave frequency ratio.

The choice of a solitary wave has been made by a few authors and is the one made in this study. Using a methodology similar to the one proposed by Zhang and Melville⁷ for infinite depth, Shen *et al.*⁸ derive a nonlinear Schrödinger equation and wave action conservation for short waves riding on a solitary wave. This confirms the suggestion by Bretherton and Garrett.⁴ They explicitly assume the perturbing wave to be a short deep water wave. They also retrieve a "wave crest" conservation equation. Wave number, wave amplitude, and frequency modulations of the short wave are thus computed along a solitary wave profile. The latter is computed by Evans and Ford's⁹ procedure. Wave number modulations along the solitary wave is an important step towards phase shift computations. Using a WKBJ perturbation method within the shallow water theory, Clamond and Germain¹⁰ allowed for solitary waves of the KdV type to coexist with short waves. Predicted short wave phase shifts are shown to agree with those measured during earlier experiments on interactions between a short monochromatic surface wave and an external solitary wave in shallow water (mean depth h_0 of 25.5 cm) by Clamond and Barthélemy.¹¹

Indeed, Clamond and Barthélemy¹¹ experimented two short waves frequencies of 1.5 and 2.3 Hz ($k_\infty h_0$ of 2.35 and 5.42 where k_∞ is the short wave wave number). They only considered the case of waves propagating in opposite direction (head-on interaction), referred to as a weak interaction. This terminology was first introduced by Miles¹² for solitary wave interactions. In contrast the case of a solitary wave propagating in the same direction (overtaking interaction) is called a strong interaction. It was shown that the surface wave train, after interaction, was phase-shifted compared to the surface wave train before. Phase shifts in this context had never been mentioned before in the literature. Previous theories or experiments on phase shift predictions dealt with sinusoidal waves.

Longuet-Higgins and Phillips¹³ showed that when two sinusoidal waves of very different wave numbers interact, the phase velocity of the shorter one will be decreased or increased (depending on the relative direction of propagation of the waves) by an amount proportional to the mass transport at the surface of the longer wave. Mass transport in solitary waves produces a small but finite displacement L of the water particles. Thus, on the same ground as Longuet-Higgins and Phillips,¹³ it is expected that short waves interacting with solitary waves will be phase shifted by the displacement. Assuming linear superposition of motion and

instantaneous displacement, the phase shift $\Delta\varphi$ undergone by the short wave is expressed by

$$\Delta\varphi = \frac{2\pi L}{\lambda} = k_\infty L, \quad (1)$$

where λ is the short-wave wave length. This heuristic formula depends on the expression of $L=L(A, h_0)$ where A is the solitary wave amplitude and h_0 is the depth of water at rest. In the present paper we discuss the relevancy of the instantaneous interaction assumption underlying (1).

Experimentally, the phase shift undergone by the short wave is measured using an harmonic analysis technique. The order of magnitude of the phase shift corresponds to a short wave time shift of 0.1 second. Determination of such a small phase shift is very sensitive to a variety of perturbing phenomena. In Clamond and Barthélemy's experiments, solitary waves had strong dispersive tails trailing the main pulse that authors claim to affect the determination of the phase shift. We improved the solitary wave generation procedure in order to minimize the undesired trailing waves. Moreover, other perturbing causes are examined.

Hereinafter, we present in Sec. II A a derivation of the wave action conservation and a new dispersion relation for first-order Stokes waves interacting with a solitary wave using a WKBJ perturbation method in the rectilinear coordinates. This approach is similar to Shen *et al.*,⁸ except that we allow for intermediate water depth and the wave crest conservation equation is simplified in order to obtain an algebraic dispersion relation. The solitary wave may be described either by the analytical solutions of Rayleigh¹⁴ or KdV¹⁵ or by Byatt-Smith's¹⁶ numerical solution. Assuming a KdV solitary wave, Clamond and Germain¹⁰ analytical expression of the phase shift is retrieved. We discuss in Sec. II B the relevance of these different solitary wave approximations in the scope of solitary wave interaction with a short wave. The theoretical results are then compared with experiments presented in Sec. III which are complementary to Clamond and Barthélemy.¹¹ Indeed, for the first time, strong interactions have been produced. Moreover, a broader range of short wave wave numbers has been examined ($k_\infty h_0$ varies from 2.73 to 7.54). In Sec. IV, the wave number modulations deduced from Sec. II A are tested through comparison with the measured phase shifts undergone by the short waves. In some cases, short waves breaking has been observed. Predictions of the maximum short wave steepness when breaking was observed are reported.

II. THEORETICAL ANALYSIS

The aim is to devise a two-dimensional (2D) model to study short surface waves modulations when the short waves ride on a solitary wave. We use a nonviscid, incompressible and homogeneous fluid with a depth at rest h_0 . We assume irrotational motions, therefore, the velocity field can be derived from a velocity potential $\Phi(x, z, t)$ and $\eta_s(x, t)$ denotes free surface displacement with respect to the rest level.

The key step is to consider a long wave which is an exact stationary solution of this flow in a reference frame moving at the wave phase speed c . To this end, the new

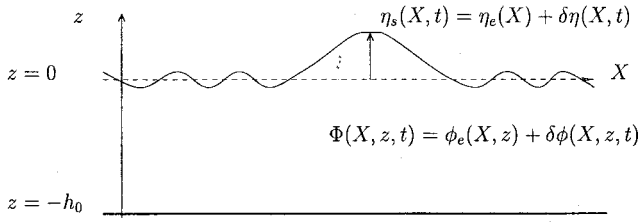


FIG. 1. Definition sketch.

horizontal variable $X = x - ct$ that describes the co-moving frame is introduced. It has long been known that this problem has an exact stationary solitary wave solution (Lavrentiev¹⁷). At the present level of derivation it is not necessary to specify its expression and we denote the velocity potential and the free surface displacement associated with this exact stationary wave by $\phi_e(X, z)$ and $\eta_e(X)$ (see Fig. 1). Other exact solutions exist, amongst which are periodic solutions.

We now seek for infinitesimal disturbances of this exact solution. The free surface elevation and velocity potential are expanded as series of a small parameter δ of the following form:

$$\eta_s(X, t) = \eta_e(X) + \delta\eta(X, t), \quad (2)$$

$$\Phi(X, z, t) = \phi_e(X, z) + \delta\phi(X, z, t). \quad (3)$$

As in the Stokes theory, δ is known to be proportional to the short wave surface slope. Assuming that the perturbation is sinusoidal in time of high-frequency ω and that its amplitude a is small compared to both its wavelength λ and depth h_0 , the first-order then reduces to a classical set of linear partial differential equations. The perturbation potential $\phi(X, z, t)$ is a harmonic function and the bottom is impermeable. The free surface displacement for the perturbation is given by

$$\eta(X, t) \times G(X) = i\omega\phi - (u_e - c) \frac{\partial\phi}{\partial X} - v_e \frac{\partial\phi}{\partial z}, \quad (4)$$

where $u_e = \phi_{eX}$, $v_e = \phi_{eZ}$ and $G(X) = g + (u_e - c)v_{eX} + v_e v_{eZ}$ written on $z = \eta_e(X)$. One recognizes $G(X)$ to be the effective gravity introduced by Longuet-Higgins and Stewart¹ and later Bretherton and Garrett.⁴ The effective gravity is the sum of the gravity and vertical acceleration at the free surface.

The free surface kinematic condition in addition to Bernoulli's relation leads to the following equation for the perturbation velocity potential at the free surface $z = \eta_e(X)$:

$$\begin{aligned} a_e(X)\phi + b_e(X) \frac{\partial\phi}{\partial X} + c_e(X) \frac{\partial\phi}{\partial z} + d_e(X) \frac{\partial^2\phi}{\partial X \partial z} \\ + e_e(X) \frac{\partial^2\phi}{\partial X^2} + f_e(X) \frac{\partial^2\phi}{\partial z^2} = 0, \end{aligned} \quad (5)$$

with

$$\begin{aligned} a_e(X) &= -\omega^2 - i\omega \left(u_{eZ} \eta_{eX} - v_{eZ} - \frac{(u_e - c)}{G(X)} [G_X \right. \\ &\quad \left. + \eta_{eX} G_z] \right), \\ b_e(X) &= -G(X) \eta_{eX} + (u_e - c)(u_{eX} - v_{eZ} + 2u_{eZ} \eta_{eX} \\ &\quad - (u_e - c)[G_X + \eta_{eX} G_z]) - 2i\omega(u_e - c), \\ c_e(X) &= G(X) - v_e(v_{eZ} - u_{eZ} \eta_{eX}) - (u_e - c) \left(\frac{v_e}{G(X)} [G_X \right. \\ &\quad \left. + \eta_{eX} G_z] - v_{eX} - \eta_{eX} v_{eZ} \right) \\ &\quad - i\omega[v_e + \eta_{eX}(u_e - c)], \\ d_e(X) &= (u_e - c)[v_e + (u_e - c) \eta_{eX}], \\ e_e(X) &= (u_e - c)^2, \\ f_e(X) &= v_e(u_e - c) \eta_{eX}. \end{aligned}$$

A. The WKBJ approximation

Length scales associated with the perturbation are assumed to be very small compared with the length scales of the long wave. The short wave is continuously adapting its characteristics to maintain itself as a high-frequency monochromatic wave. This assumption of WKBJ type is equivalent to that of Shyu and Phillips.¹⁸ A small parameter $\mu = \lambda/\Lambda$ (where λ is the short wave wavelength and Λ is a characteristic length of the solitary wave) is naturally involved and a new variable $X^* = \mu X$ is introduced. The WKBJ approximation postulates slow variations of the amplitude $\mathcal{A}(X, z)$ and rapid variations in the phase $S(X, z)$. This is written in the following form:

$$\phi^*(X^*, z) = \mathcal{A}^*(X^*, z) e^{iS^*(X^*, z)/\mu}, \quad (6)$$

where $\phi^*(X^*, z) = \phi(X, z)$ and $\mathcal{A}^*(X^*, z) = \mathcal{A}(X, z)$ and $S^*(X^*, z) = \mu S(X, z)$ are real numbers. The amplitude and phase are expanded in even series of μ of the form

$$\mathcal{A}^*(X^*, z) = \mathcal{A}_0^*(X^*, z) + \mu^2 \mathcal{A}_2^*(X^*, z) + \dots + \mathcal{O}(\mu^{2n}), \quad (7)$$

$$S^*(X^*, z) = S_0^*(X^*, z) + \mu^2 S_2^*(X^*, z) + \dots + \mathcal{O}(\mu^{2n}). \quad (8)$$

At the lowest orders (μ^{-2} and μ^{-1}), the only nontrivial relation is $S_0^* = S_0^*(X^*)$. The modulated wave number $k(X) = S_{0X^*}^*$ is then introduced.

Depending on the relative scale of μ and δ , Eq. (5) will simplify differently. Indeed, when $\mu \sim \delta$ orders corresponding to μ and δ cannot be separated. Dingemans¹⁹ reports studies of the refraction of waves by currents for which vertical dependency predominates over horizontal and temporal variations by assuming $\mu \ll \delta$. Regarding the interaction problems, the correct assumption is $\mu \gg \delta$ as made by Mei²⁰ to study the refraction of waves on slowly varying currents. The main difference here with the available literature is not to assume that the long wave is a linear one either in finite

TABLE I. First two orders in μ of the coefficients in (5) and of the effective gravity $G(X)$.

	$\mathcal{O}(1)$	$\mathcal{O}(\mu)$
$a_e(X)$	$-\omega^2$	$i\omega v_{ez}$
$b_e(X)$	$-2i\omega(u_e - c)$	$-g\eta_{eX} + (u_e - c)(u_{eX} - v_{eZ})$
$c_e(X)$	g	$i\omega[v_e + (u_e - c)\eta_{eX}]$
$d_e(X)$	0	$(u_e - c)[v_e + (u_e - c)\eta_{eX}]$
$e_e(X)$	$(u_e - c)^2$	0
$f_e(X)$	0	0
$G(X)$	g	0

depth or in infinite depth. Moreover, most authors have focused on amplitude modification and Doppler shift. In contrast, we will analyze the phase shift of the short wave. Our approach also differs from that of Clamond and Germain¹⁰ since they explicitly assumed a solution in the small amplitude approximation. In contrast, the exact solitary wave solution we consider can be of large amplitude. However, the coefficients of Eq. (5) contain terms of different orders in $\sigma = h_0/\Lambda$, that can be sorted out. The two leading orders are given in Table I.

Assuming $\sigma \sim \mu$ ($\lambda \sim h_0$), the perturbation fulfills the following dispersion relation obtained by considering the order μ^0 :

$$\Omega^2 = gk(X) \tanh[k(X)(\eta_e(X) + h_0)]. \quad (9)$$

It appears that the effective gravity reduces to gravity. The wave action conservation is retrieved at the order μ^1

$$\left[\frac{a^2(C_g + c - u_e(X))}{\Omega} \right]_X = 0, \quad (10)$$

with $\Omega = \omega - k(X)(u_e(X) - c)$, $a = \mathcal{A}_0\Omega/g$ the short wave amplitude at the first order and $C_g = d\Omega/dk$ the intrinsic group velocity. The dispersion relation (9) for given $u_e(X)$, $\eta_e(X)$ and c is solved numerically for $k(X)$ using a Newton–Raphson method.

We briefly discuss qualitative behaviors. At $x = \pm\infty$ the short wave has a constant wave number k_∞ , the one observed in the laboratory. Note that (9) differs from the dispersion relation obtained for refraction on a slowly varying current. Indeed, changes in depth as the short wave rides on the long wave are embedded in (9) since $(\eta_e(X) + h_0)$ appears instead of h_0 alone. The phase shift $\Delta\varphi$ is easily computed when the modulated wave number $k(X)$ is obtained. It reads

$$\Delta\varphi = \int_{-\infty}^{+\infty} (k(X) - k_\infty) dX, \quad (11)$$

where $k(X)$ is the wave number in the physical space.

Assuming a solitary wave solution of KdV type, the basic state reads

$$\eta_e(X) = \epsilon f(X) h_0, \quad (12)$$

$$u_e(X) = \epsilon c f(X), \quad (13)$$

$$c = c_0(1 + \epsilon/2), \quad (14)$$

with $\epsilon = A/h_0$, $f(X) = \text{sech}^2(\beta X/2)$, $\beta/2 = \sqrt{3\epsilon/4h_0^2}$ and $c_0^2 = gh_0$. We also assume that the wave number expands as a series of ϵ

$$k(X) = k_\infty + \epsilon k_1 + \mathcal{O}(\epsilon^2). \quad (15)$$

Expansions of the right and left-hand side of Eq. (9) in series of ϵ including the first two leading orders yield

$$\Omega^2 = (\omega + k_\infty c_0)^2 + \epsilon[2c_0(\omega + k_\infty c_0)(k_1 - k_\infty f)] + \mathcal{O}(\epsilon^2), \quad (16)$$

$$gk \tanh(k(\eta_e + h_0)) = gk_\infty \tanh(k_\infty h_0) + \epsilon[gk_1 \tanh(k_\infty h_0) + gk_\infty h_0(k_1 + k_\infty f)(1 - \tanh^2(k_\infty h_0))] + \mathcal{O}(\epsilon^2). \quad (17)$$

At the lowest order, formula (9) together with (16) and (17) provides the undisturbed dispersion relation for $X = \pm\infty$

$$(\omega + k_\infty c_0)^2 = gk_\infty \tanh(k_\infty h_0). \quad (18)$$

At the next order (ϵ), formula (9) gives

$$\frac{k_1}{k_\infty} = \Gamma f(X), \quad (19)$$

with $\Gamma = (c_0 + \omega_{\text{lab}}/2k_\infty - c_g)/(c_0 + c_g)$ where $c_g = d\omega_{\text{lab}}/dk_\infty$ and $\omega_{\text{lab}}^2 = (\omega + k_\infty c_0)^2$. The phase shift (11) then reads

$$\Delta\varphi = \epsilon k_\infty \Gamma \int_{-\infty}^{+\infty} f(X) dX. \quad (20)$$

We retrieve in a more general framework the phase shift $\Delta\varphi_{\text{KdV}}$ given by Clamond and Germain¹⁰

$$\frac{\Delta\varphi_{\text{KdV}}}{k_\infty h_0} = \frac{4}{\sqrt{3}} \Gamma \sqrt{\frac{A}{h_0}}. \quad (21)$$

We may note that Γ tends to 1 when the short wave frequency increases.

B. Short wave modulation for different solitary wave solutions

At this level, the exact solitary wave solution (basic state around which a perturbation is sought) is not specified to obtain (9) and (10). A different solitary wave approximation may be used, as long as the terms neglected in Eq. (5) using this approximation are at least an order of magnitude smaller than the perturbation contribution. This is required so that the basic flow and the perturbation can be solved separately. The numerical solution proposed by Byatt-Smith¹⁶ will easily fulfill this assumption, as the error allowed when computing it can be less than 10^{-4} on the free surface elevation whereas the short wave amplitude is of order 10^{-2} . We compute Byatt-Smith numerical solution up to $A/h_0 = 0.7165$ using the accurate and efficient algorithm devised by Byatt-Smith and Longuet-Higgins.²¹ The accuracy of Byatt-Smith numerical solution is checked against measurements of both free surface elevation and phase speed [see Figs. 2 and 3(a)]

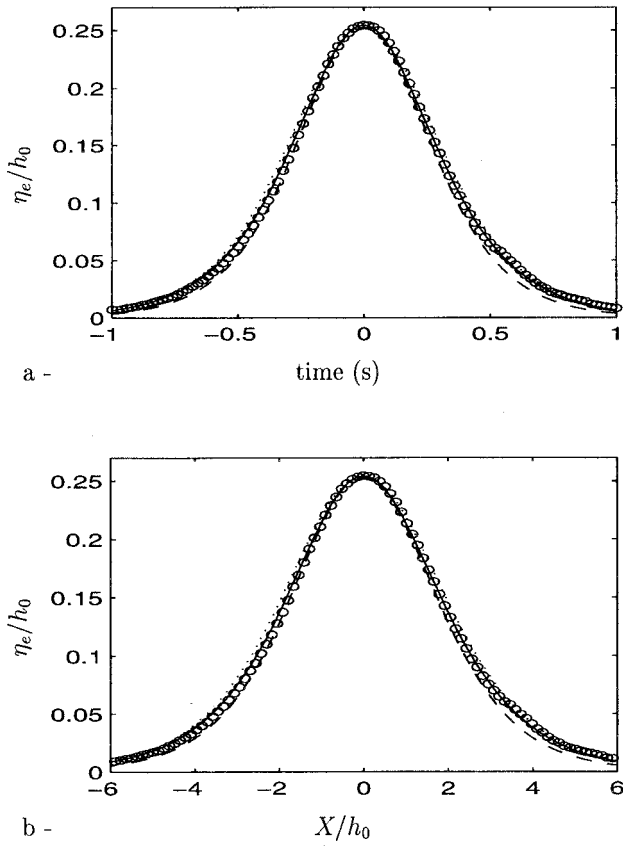


FIG. 2. Dimensionless free surface elevation at one location vs time (a) and in the steady reference frame (b) obtained for Byatt-Smith's numerical solution (—), KdV (- -), or Rayleigh's (· · ·) analytical solutions and experiments (○).

for $A/h_0 \leq 0.5$. Indeed, we were not able to produce larger solitary wave because of the device capabilities (see Sec. III).

We shall also consider analytical solutions (which are not strictly speaking exact solutions) including the KdV or shallow water approximation, which rely on both long waves and small-amplitude assumptions (weakly nonlinear theory). Within the shallow water theory, all series expand in either even or uneven powers of $\epsilon = A/h_0$. This means that the order of magnitude that separates two consecutive approximations is at least ϵ^2 . Accordingly if first-order approximation is of order 1, corrections to obtain a second-order approximation will be of order ϵ^2 . Between 1 and ϵ^2 , we ought to be able to solve separately the perturbation first order ($\sim \delta = ak$) leading to (9) and giving the rapid variation of the phase, and the second-order ($\sim \delta\mu$) leading to (10) and describing the slow variations in the amplitude of the perturbation. This means that it is necessary for $\epsilon^2 \ll \mu\delta$, which can be met in the KdV domain of validity when ϵ is less than 0.15.

Avoiding the latter restriction of small amplitude, namely allowing ϵ to be of order 1 (strongly nonlinear theory), Rayleigh¹⁴ derived the following solitary wave solution, reported by Lamb²² (Sec. 252):

$$\eta(x,t) = A \operatorname{sech}^2[\beta(x-ct)/2], \quad (22)$$

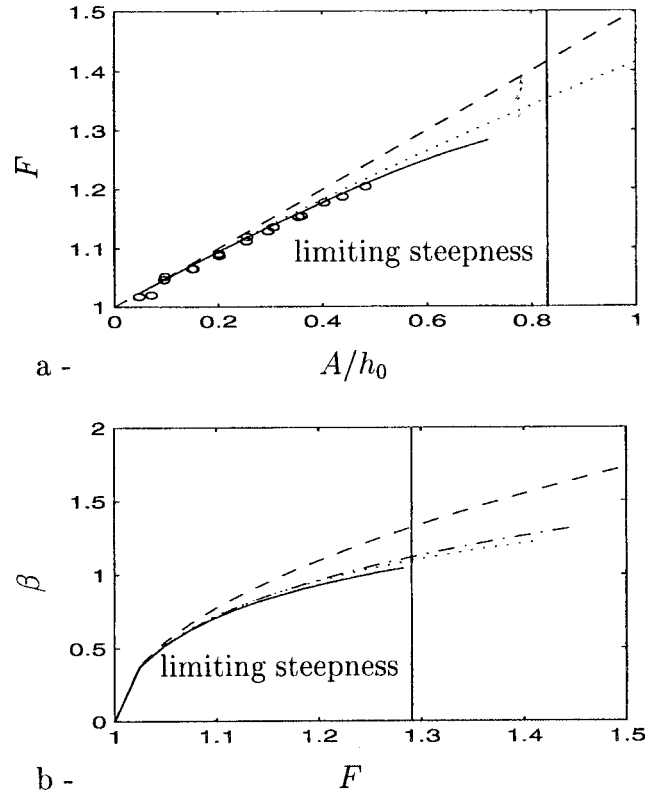


FIG. 3. Froude number $F = c/\sqrt{gh_0}$ vs solitary wave dimensionless amplitude A/h_0 (a) and outskirts decay coefficient β vs Froude number (b) obtained for Byatt-Smith's numerical solution (β is then the Stokes outskirts decay coefficient solution of the relation $F^2 = \tan(\beta)/\beta$) (—), KdV (- -), or Rayleigh's (· · ·) analytical solutions and experiments (○).

$$\frac{\beta}{2} = \sqrt{\frac{3A}{4h_0^2(h_0+A)}}, \quad (23)$$

$$c = \sqrt{g(h_0+A)}, \quad (24)$$

with the depth-averaged velocity given by

$$\bar{u}(x,t) = c \left(1 - \frac{h_0}{h_0 + \eta(x,t)} \right), \quad (25)$$

and the horizontal and vertical velocity given by

$$u(x,z,t) = \bar{u} + \frac{(\eta+h_0)^2}{6} \bar{u}_{xx} - \frac{(z+h_0)^2}{2} \bar{u}_{xx}, \quad (26)$$

$$v(x,z,t) = -\bar{u}_x(h_0+z). \quad (27)$$

This is the steady solution of the set of equations proposed by Serre²³ and later by Su and Gardner²⁴ in a strongly nonlinear framework.

Since we assume $\sigma \sim \mu$ and in order to be consistent with our WKB perturbation method, the horizontal velocity at the free surface $u_e(X, \eta_e)$ will be taken equal to \bar{u} when truncating terms of order μ^2 and higher in (5) for Rayleigh and KdV approximations. For Byatt-Smith exact numerical solution, since this order separation is not possible, $u_e(X, \eta_e)$ will be taken equal to the full free surface horizontal velocity contribution. Moreover, separating orders, we require that $\sigma^4 \ll \mu\delta$, which means $\delta \gg \sigma^3$. This condition will be fulfilled in the experiments.

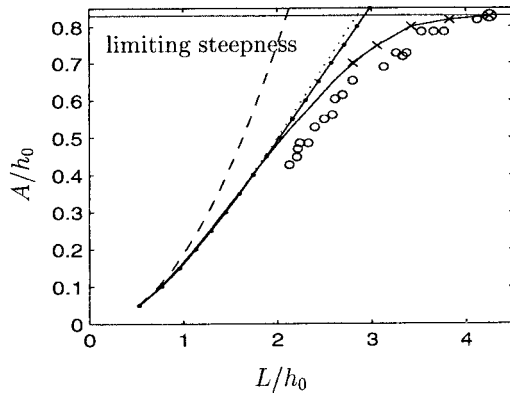


FIG. 4. Solitary wave dimensionless amplitude vs horizontal displacement at the free surface obtained from Byatt-Smith's (—) numerical solution complemented by (×) ninth-order theory of Fenton (Ref. 26) (⊗) calculation by Longuet-Higgins (Ref. 27), Rayleigh free surface velocity (—), formula (30), i.e., Rayleigh (⋯) and KdV (---) depth-averaged velocities and experiments from Longuet-Higgins (Ref. 25) (○).

As mentioned in the Introduction, the short wave phase shift can be deduced heuristically from the particle displacement L at the free surface of the solitary wave. The particle displacement L at the free surface is defined in general by

$$L = 2 \int_0^\infty \frac{c - u(x, \eta)}{u(x, \eta)} dx, \quad (28)$$

where $u(x, \eta)$ denotes the horizontal velocity at the solitary wave free surface in the co-moving frame and c is the solitary wave phase speed.

In the Korteweg and De Vries¹⁵ approximation, the horizontal velocity at the free surface is the mean horizontal velocity and L is given explicitly by

$$L = \frac{4}{\sqrt{3}} h_0 \sqrt{\frac{A}{h_0}}. \quad (29)$$

Thus, we note that formula (21) tends to the heuristic formula (1) where L is given by (29) for high-frequency short wave. For large amplitude solitary waves ($0.4 \leq A/h_0 \leq 0.7$), Longuet-Higgins²⁵ showed that formula (29) is rather inaccurate and underestimates the horizontal displacement by 25% to 40%. However, it is still possible to derive from Rayleigh and Byatt-Smith velocities at the free surface other estimations for L to be included in the heuristic formula (1). We shall also consider an approximation for L based on the depth averaged velocity \bar{u} of Rayleigh solution, which lead to the following analytical expression for L :

$$L = \frac{4}{\sqrt{3}} h_0 \sqrt{\frac{A}{h_0} \left(1 + \frac{A}{h_0} \right)}. \quad (30)$$

On Fig. 4, we plot these estimations of L , together with Longuet-Higgins²⁵ experiments. We also report on Fig. 4 Fenton²⁶ ninth-order theory and Longuet-Higgins²⁷ calculations for large amplitude solitary waves up to the limiting steepness ($0.7 \leq A/h_0 \leq 0.8332$). We also report this limiting steepness on the plots of the Froude number versus solitary wave amplitude [Fig. 3(a)] and of the outskirts decay coefficient versus the Froude number [Fig. 3(b)].

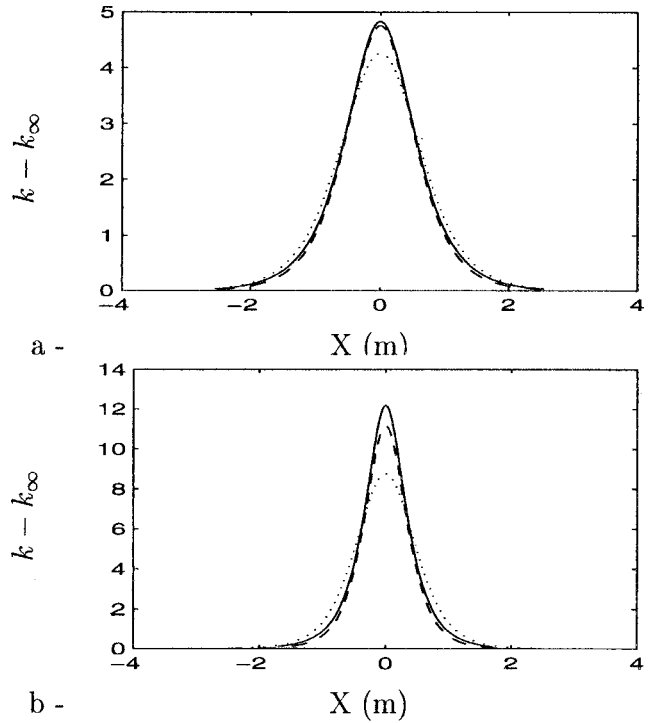


FIG. 5. Wave number modulations along the solitary wave ($X=0$ at the solitary wave crest) predicted by WKBJ theory for the strong interaction of a 2 Hz shortwave ($k_x = 16.09$, $h_0 = 0.3$ m) and a solitary wave of amplitude $A/h_0 = 0.2025$ (a) and $A/h_0 = 0.4129$ (b) given by Byatt-Smith's numerical solution (—), KdV (---), and Rayleigh (⋯).

It is clear that displacements at the free surface derived from Rayleigh free surface velocity or even Rayleigh depth-averaged velocity are very accurate for a broader range of solitary wave amplitude than KdV. Up to $A/h_0 = 0.4$, displacements derived from the free surface velocity from Byatt-Smith's exact solution, Rayleigh's analytical solution and displacements derived from Rayleigh depth-averaged velocity merge, whereas displacement derived from KdV's solution are much smaller since $A/h_0 = 0.15$. For $A/h_0 \geq 0.4$, some discrepancies appear between the simplified expression (30) and estimation of L obtained either from the free surface velocity of Rayleigh or the numerical solution from Byatt-Smith. However, up to $A/h_0 = 0.7$ the deviation between formula (30) and Byatt-Smith is less than 10% whereas it reaches 40% between formula (29) and Byatt-Smith. Besides, in the same range, the deviation between (30) and Longuet-Higgins' experiments is at most of 20%. Part of this deviation might be due to a suspected bias in Longuet-Higgins measurements owing to the added displacement caused by a secondary hump following the solitary wave. Using formula (30) in the heuristic approach we overcome the small amplitude KdV limit and short wave phase shift is given analytically by

$$\frac{\Delta \varphi_H}{k_x h_0} = \frac{4}{\sqrt{3}} \sqrt{\frac{A}{h_0} \left(1 + \frac{A}{h_0} \right)}. \quad (31)$$

Indeed, we show by comparing the free surface displacement derived from the numerical solution of Byatt-Smith and the displacement obtained from Rayleigh depth-averaged ve-

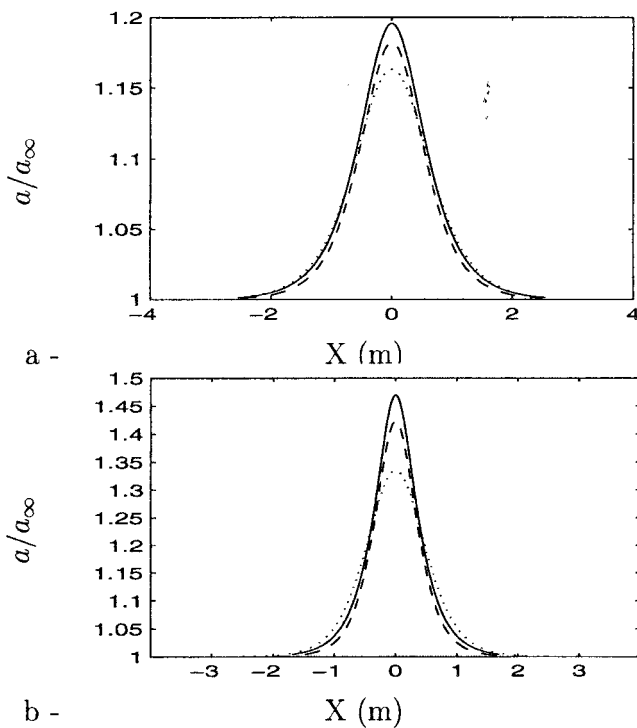


FIG. 6. Amplitude modulations (same legend as Fig. 5).

locity that this simple formula accurately reproduce the heuristic approach for solitary waves up to $A/h_0=0.4$ and with less than 10% error up to $A/h_0=0.7$.

Finally, we have to compare the amplitude and wave number modulation obtained using each analytical approximation of the solitary wave and the numerical solution. Wave number modulations (Fig. 5) associated with KdV show better agreement than Rayleigh with the modulations obtained using Byatt-Smith's numerical solution. In all cases, the highest maximum wave number modulations are given using Byatt-Smith, with Rayleigh giving the lowest. The deviation between Rayleigh and Byatt-Smith at the maximum of wave number modulations reaches 40% for $A/h_0=0.5$ in strong interaction. With respect to amplitude modulations (Fig. 6), the deviation between Byatt-Smith and Rayleigh ranges from the double to four times the deviation between Byatt-Smith and KdV when solitary wave amplitude increases. Yet, Byatt-Smith predicts amplitude modulation at the solitary wave peak that are less than 6% greater than KdV (for $A/h_0=0.5$ in strong interaction). As a consequence of both wave number and amplitude modulations, when comparing steepness maxima at the crest of the solitary wave [Figs. 7(a) and 7(b)], KdV and Byatt-Smith give close results up to $A/h_0=0.3$. For $A/h_0 \geq 0.3$, predicted steepness maxima are smaller for KdV than for Byatt-Smith. In all cases, using Rayleigh's solution, predicted steepness maxima are smaller. Yet, the phase shifts deduced from wave number modulations given by Rayleigh are in better agreement with Byatt-Smith than KdV, as shown in Figs. 7(c) and 7(d). This is in line with our conclusion on particles displacements at the free surface. We suggest this is due to the better description of both the outskirts decay coefficient and the phase speed in Rayleigh solution [see Figs. 3(a) and 3(b)].

As a conclusion, granted that Byatt-Smith's numerical solution is the exact solitary wave solution required in the theory, Rayleigh's approximation appears to be better than KdV's to test the short wave phase shift in the interaction with a solitary wave. But regarding Doppler effects and particularly steepness prediction at the solitary wave crest, KdV would give a better approximation than Rayleigh.

III. EXPERIMENTAL PROCEDURE

The experiments are conducted in a 36 m long, 0.55 m wide, and 1.2 m high flume as sketched out on Fig. 8. It is equipped with two wave makers.

At one end of the flume a piston wave paddle can be displaced horizontally. The piston is linked to a hydraulic jack capable of a 600 mm stroke. The control system is monitored by a computer. Different motions of the paddle can be prescribed by the computer, enabling the generation of either solitary waves or sinusoidal waves. This ability was used for strong interactions when solitary waves and short waves need to be generated at the same end of the flume. Nevertheless the piston type wave maker, although not perfect, is more appropriate for long wave generation rather than for short wave generation since it displaces the whole water column uniformly. Ideally, the piston would need to flex in such a manner as to reproduce the solitary wave vertical distribution of the velocity. This is not possible with our wave maker. However, we need to prescribe an appropriate law of motion for the paddle in order to produce solitary waves that are as pure as possible. Clamond and Germain¹⁰ used a law deduced from the first-order shallow water theory. All solitary waves generated with this motion exhibit a main pulse followed by a dispersive tail with no more than 10% of the amplitude of the leading pulse. In order to decrease the amplitude of the dispersive tail, different laws of motion for the piston wave maker were tested. It appears that solitary waves generated using a paddle motion law conforming to (25) are purer (smaller dispersive tail than with the original law) and more rapidly established. Moreover, by reproducing different experiments concerning solitary wave generation with any generation law, we assess that it is highly reproducible. So that for a given paddle law, we could know the solitary wave amplitude at any location in the flume given the probe accuracy. The law deduced from the Rayleigh solution implies larger paddle displacement than other laws. With regard to the finite stroke of the jack, this latter law lead to smaller solitary wave amplitudes. For a water depth of $h_0=0.3$ m the upper bound of the solitary wave dimensionless amplitude is 0.35 while the first-order shallow water law allows a dimensionless amplitude up to 0.5.

For weak interactions, a plunging wedge wave maker was used to generate high-frequency monochromatic sinusoidal waves. It is driven through a scotch-yoke (Welt²⁸) by an electric motor rotating at constant speed. The frequency of the wedge motion ranges from 1 to 10 Hz. The amplitude of the motion is adjusted by prescribing a fixed eccentricity. This wave maker can be located at will anywhere along the flume. For the set of weak interactions, it was located at 28 m from the piston wave maker.

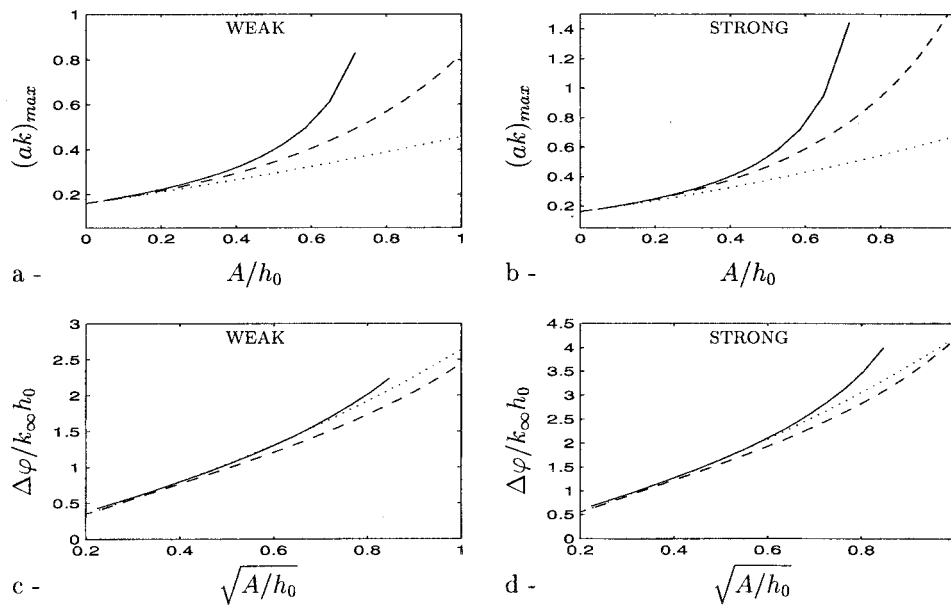


FIG. 7. (a) and (b) Steepness maxima at the crest of the solitary wave and (c) and (d) phase shifts deduced from wave number modulations predicted by WKBJ theory for weak and strong interaction of a 2 Hz short wave ($k_\infty=16.09$, $h_0=0.3$ m) of amplitude 1 cm and a solitary wave given by Byatt-Smith's numerical solution (—), KdV (- -), and Rayleigh (· · ·).

The depth at rest was fixed throughout the experiments at $h_0=0.3$ m. It is a compromise between the capabilities of the solitary wave wave maker and the high frequency wedge wave maker. In addition for this depth the short wave has a dimensionless wave number $k_\infty h_0$ ranging from 2.73 to 7.54 for frequencies varying from 1.5 to 2.5 Hz. It indicates that experiments were performed for intermediate to deep water depths conditions. The short wave is in fact a wave group as shown on Fig. 9(a). The front part is highly unstable. Envelope solitons can be generated in this front part and at least strong modulations of the amplitude are systematically observed. The central part of the record [Fig. 9(b)] shows a slight modulation in amplitude along with an asymmetry between crests and troughs due to second-order nonlinearities. Harmonic analysis of this central zone shows that the first harmonic component is a very small fraction of the fundamental component. Thus it is considered to be a nearly pure monochromatic wave. Care is taken so that the measurement of the interaction is made in the central part. Over 2.5 Hz the wave is severely damped and propagates no further than 3 m away from the plunging wave maker. It was noticed during

the experiments that damping was less pronounced after the tank had just been refilled, in other words when the free surface was clean. We thus attributed this damping to the free surface contamination, as Van Dorn²⁹ already suggested. Thus, as it is not possible, given the size of the tank, to maintain the free surface clean enough, we did not proceed over 2.5 Hz.

Surface displacements during the experiments on the interaction between short surface waves and surface solitary waves are measured in fixed locations by resistive probes. Probe precision was estimated at 0.5 mm for free surface elevations lower than 5 cm and at 1 mm beyond this limit. This is due to probe calibration. These probes are combined in arrays and the distance between probes is fixed. The array can be moved along the flume, between 11 and 22 m from the piston wave maker depending on the experimental conditions. An extra probe can be dedicated to the measurement of the solitary wave before it has interacted. All experimental recordings of interactions are measurements of free surface displacement against time (between 15 and 25 seconds duration). The probes are located along the center line of the

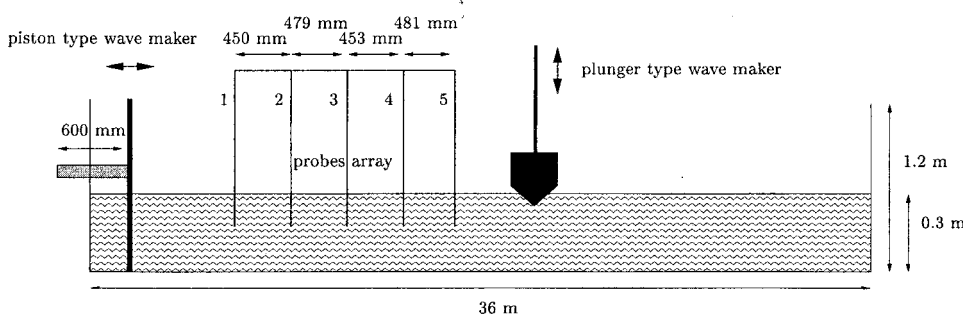


FIG. 8. Sketch and dimensions of the experimental equipment.

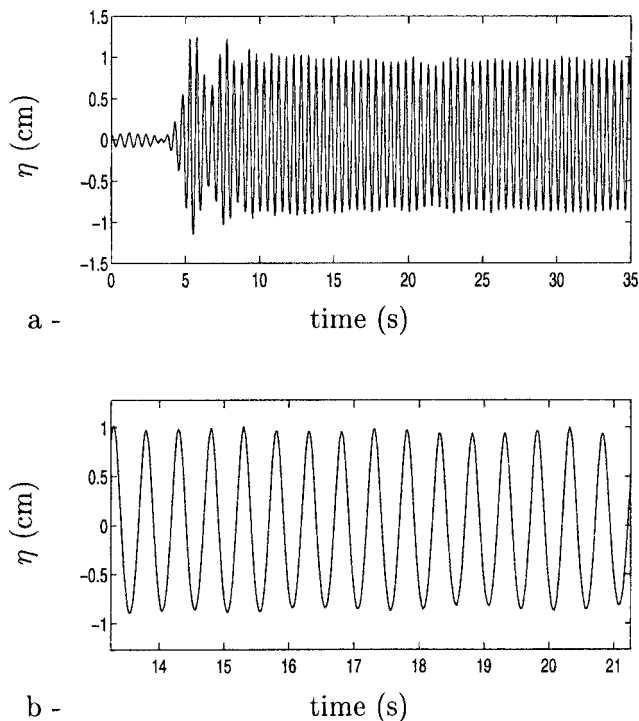


FIG. 9. Recording of a high-frequency wave group at 10 m from the wedge wave maker; $f=2$ Hz, $h_0=0.3$ m. (b) is a close-up of the recording plotted in (a) showing evidence of second-order contribution.

flume to avoid lateral perturbations. We generate a solitary wave of amplitude A , a short wave of frequency f (wave number k_∞), and of amplitude a_∞ . A typical example of an interaction is presented on Fig. 10, on which four zones can be differentiated. Zone A is the recording of the short wave before interaction, zone B is the recording of the interaction between the solitary wave and the short wave when the solitary wave contribution is predominant, and zone C is the recording of the short wave after it has interacted. The slight modulation is due to the dispersive tail trailing the soliton. Zone D is a useless part of the recording. Indeed the reflected solitary wave interacts with the dispersive tail and the short wave.

From the theoretical point of view, we know that the short wave undergoes wave number modulations during the interaction. The modulations are difficult to obtain directly from the measurements. However, phase shift of the wave train A with respect to the wave train B is a consequence of

wave number modulations. The data processing to obtain this phase shift is based on a harmonic analysis technique detailed in Clamond and Barthélemy.¹¹ This was found to be the most precise method. The methodology was tested on pure synthetic sinusoidal signals with no other contribution. In this case the phase shift between two arbitrary zones with such signals is 0 since no other wave is present. This method applied to such signals yields a phase shift as low as the machine roundoff error in double precision, namely 10^{-16} rad. Concerning our experiments, we also tested the error induced by the dispersive tail that follows the solitary wave main pulse in zone C. To this end, two tests have been considered. First, we apply harmonic analysis to the superposition of a pure synthetic sinusoidal signal and a measured free surface elevation for a single solitary wave. We considered solitary waves generated by the different paddle motion laws we tested. But in the whole range of solitary wave amplitude, the improvements in reducing the dispersive tail did not show a significant reduction in phase shift error due to inaccuracy in the method because of the dispersive tail. This error is at most 0.1 rad. Second, all interaction experiments were repeated with solitary waves generated either with Rayleigh or KdV paddle motion law. Phase shifts obtained from one or the other experiment series do not separate more than the error than can be estimated for a single experiment. Indeed a large contribution to the error comes from irregularities in the measured short wave signals. This was assessed by the following test. A record of a freely propagating short wave is split in two. Phase shift between both parts is computed. This was repeatedly done and it was found that phase shifts could reach 1.5 rad without any apparent disturbances. This error in phase computation is mainly attributed to uncertainties in the frequency determination of short signals (records less than 10 s). The reliability of the frequency of the wave maker was checked. It was felt that the best way to estimate and reduce errors in phase shift determination was to repeat the measurements. All the phase shifts presented in this section are, therefore, an average on 5 or 6 values obtained at locations spanning 2 m (probe array). All the values presented fulfilled the criteria of an error lower than 1 rad, estimated from two times the standard deviation of the 5 or 6 values. Experiments for which this criteria was not fulfilled have been excluded. More details regarding experimental errors can be found in Guizien.³⁰ As mentioned above, given a short wave frequency and a solitary wave

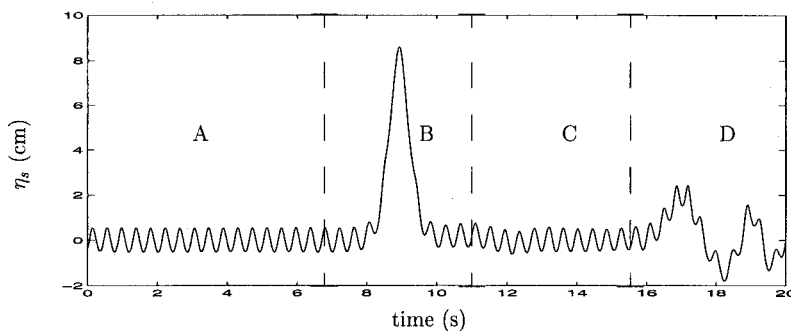


FIG. 10. Free surface elevation against time at 19.423 m from the piston wave maker; for the solitary wave $A/h_0=0.3$ and the frequency of the short wave is $f=2.5$ Hz ($k_\infty=25.15$) for an amplitude of $a_\infty=5.7$ mm ($h_0=0.3$ m).

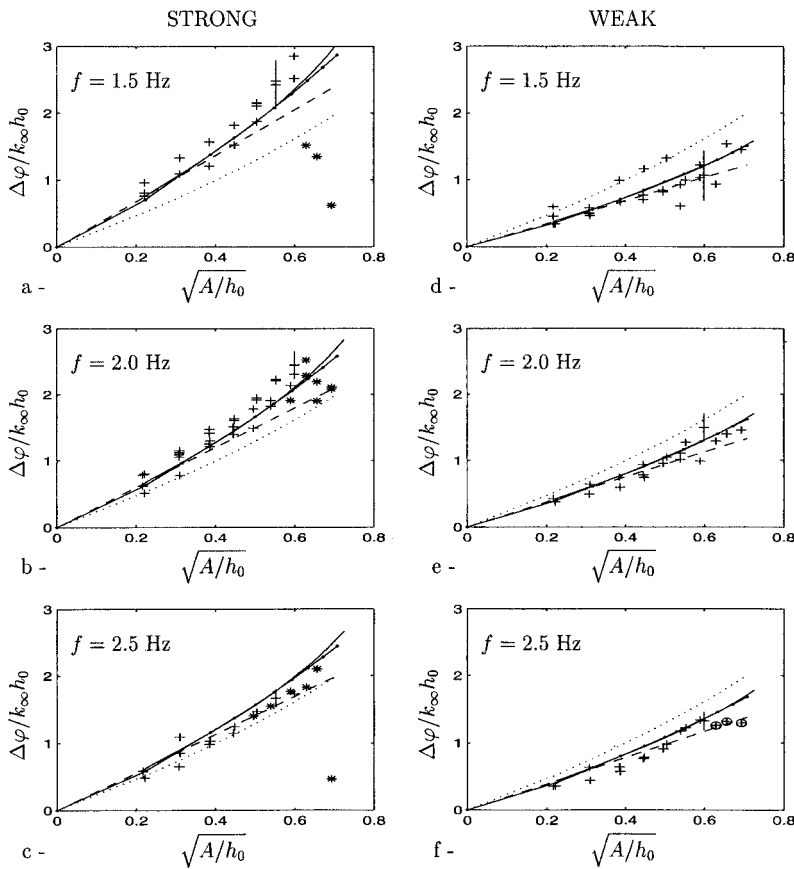


FIG. 11. (+) Experimental phase shifts versus the square root of solitary wave dimensionless amplitudes; (· · ·): $\Delta\varphi_H$; (—): $\Delta\varphi_R$; (- -): $\Delta\varphi_{KdV}$; (- · -): $\Delta\varphi_{BS}$; (*): short wave was observed breaking; (O): short wave suspected to be breaking from pictures; (a) strong and (d) weak: $f=1.5$ Hz; (b) strong and (e) weak: $f=2.0$ Hz; (c) strong and (f) weak: $f=2.5$ Hz with $h_0=0.3$ m.

amplitude, we carried out experiments for the different solitary wave laws of generation, considered as repetition of the same experiments. Besides, the short wave amplitude was also allowed to vary, from 4 to 12 mm, as long as the short wave out of the interaction was stable.

IV. RESULTS AND DISCUSSION

The interaction between a surface solitary wave and a short wave can be analyzed using very simple arguments, as recalled in the introduction. The short wave phase shift is then given by formula (31). We emphasize that this formula is obtained by considering only displacement due to solitary waves, linearly and instantaneously. As a consequence, the short wave direction of propagation is not taken into account. It should be noted that (31) is independent of the short wave amplitude a_∞ . Figure 11 shows the experimental results of nondimensional phase shifts $\Delta\varphi/(k_\infty h_0)$ against $\sqrt{A/h_0}$ for strong and weak interactions and various short wave frequencies. We do not identify on the plots of Fig. 11 the short wave amplitude. Indeed, it was not possible to show experimentally any dependency of the short wave phase shift on the short wave amplitude.

Heuristic phase shift $\Delta\varphi_H$ given by formula (31) is plotted as a dotted curve. In this representation, it is the same curve in all cases. Experimentally, weak interactions give smaller phase shifts than $\Delta\varphi_H$ while strong interactions give larger ones. Moreover it appears that for strong interactions the higher the frequency of the short wave, the closer the nondimensional experimental phase shifts are to

$\Delta\varphi_H/(k_\infty h_0)$. This is not surprising since formula (31) assumes that the short wave does not propagate during the interaction. Indeed, this assumption is met with decreasing error as the frequency increases since then the short wave phase velocity also decreases. For weak interactions, since the induced phase shifts are smaller, it remains difficult to observe this effect as clearly. In order to clearly show this argument, we plot on Fig. 12 the relative deviation between phase shifts given by formula (31) and experimental values or formula (9) for a Rayleigh solitary wave as the short wave wave number increases. In fact, this graph shows that the relative error one would do when using formula (31) to estimate the short wave phase shift, decreases when the short wave frequency increases. This error is less than 10% when

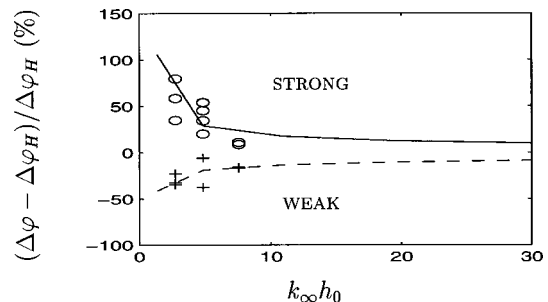


FIG. 12. Relative deviation between phase shifts given by formula (31) and experimental values for (O): strong interaction; (+): weak interaction and given by formulas (31) and (9) for a Rayleigh solitary wave for (—): strong interaction; (---): weak interaction.

$k_{\infty}h_0 \geq 30$. However, the departure of $\Delta\varphi_H$ from the dimensional phase shift increases when the short wave frequency increases as shown by Clamond and Germain.¹⁰ This is because the wave number increases more rapidly than the phase velocity decreases with increasing frequency.

On Fig. 11 we also plot the phase shifts $\Delta\varphi_{\text{KdV}}$ given by formula (21), $\Delta\varphi_R$ given by formula (9) for a Rayleigh (*R*) solitary wave and $\Delta\varphi_{\text{BS}}$ given by formula (9) for a Byatt-Smith (*BS*) solitary wave. Up to $A/h_0 = 0.15$, formulas (21) and (9) give very close results, which is in agreement with the KdV theory limit. Indeed, we already showed in Sec. II A how (9) reduces to (21) under the small amplitude assumption. Formula (9) for a Rayleigh or a Byatt-Smith soliton allows to predict phase shifts for a wider range of solitary waves, theoretically up to the limiting dimensionless amplitude of 0.8332 (Longuet-Higgins²⁵). In our experiments, we were limited to $A/h_0 \leq 0.5$. In weak interactions, taking into account the experimental error (represented by the error bars on Fig. 11), it is not possible to conclude on a better agreement with one or the other formula. However, the advantages of this formulas appear for strong interactions when phase shifts are the largest. Indeed, the experimental results for large solitary waves in strong interaction are closer to predictions of formulas (9) (either based on the Rayleigh solitary wave approximation or Byatt-Smith numerical solution) for frequencies of 2 and 1.5 Hz. Repeated experiments (especially at 2 Hz) confirm this trend. For 2.5 Hz, this tendency is not as clear, partly due to the early breaking observed.

As a matter of fact, a 2.5 Hz short wave was observed “breaking” for a solitary wave of dimensionless amplitude $A/h_0 = 0.25$ whereas for 2 and 1.5 Hz frequencies, breaking only occurred for the largest solitary waves, respectively, for $A/h_0 = 0.4$ and $A/h_0 = 0.45$. We use here the term breaking to refer to foam patches that one can see on the free surface. This breaking is due to the steepening of the short wave when both amplitude and wave number increase. Thus, short waves of different amplitudes but with the same frequency and interacting with the same solitary wave may be differentiated by breaking, whereas if only the phase shift is considered they cannot. The maximum short wave steepness at the crest of the solitary wave when the short wave was observed breaking is computed from (9) and (10) using Byatt-Smith numerical solitary wave solution. These values bound to experimentally observed breaking are given in Table II. We also report in Table II the maximum steepness values predicted for the weak interaction with the largest solitary wave experimented ($A/h_0 = 0.5$). Breaking was never clearly observed in our weak interactions (no foam patches). Because of the uncertainty concerning the breaking limit, we may just stress that for the same predicted steepness for $f = 2.5$ Hz ($k_{\infty}h_0 = 7.54$), short waves are observed breaking in the strong interaction but not in the weak interaction case. Moreover, the predicted steepness when breaking is observed is always smaller than the Stokes limit of 0.4461 for waves propagating at rest. This all suggests that breaking is not determined only by the steepness but also by the underlying velocities.

TABLE II. Maximum short-wave steepness at the crest of the solitary wave computed from (9) and (10) when the short wave was observed breaking in strong interaction and for the largest solitary waves experimented ($A/h_0 = 0.5$) in weak interaction (the short wave was NOT observed breaking in these latter cases).

$k_{\infty}h_0$	Strong	Weak
2.73	0.267	0.189
4.83	0.320	0.296
7.54	0.150	0.535

V. CONCLUSION

Theoretically we found a dispersion relation (9) to describe the wave number modulations of a short wave riding on a solitary wave that is similar to the one obtained for the refraction of waves in slowly varying media, except that it includes free surface elevation. Wave action conservation (10) is also obtained. Any solitary wave solution may be used and, if assuming a small amplitude one, Clamond and Germain’s¹⁰ analytical expression for the phase shift undergone by the short wave is confirmed.

We compare short wave wave number and amplitude modulations obtained from (9) and (10) when using Byatt-Smith’s numerical solution and KdV or Rayleigh’s analytical solutions. The shape of the wave number modulation curve associated with KdV appears to be closer than Rayleigh to the one obtained with Byatt-Smith, but it misses the maximum that occurs at the crest of the solitary wave for large solitary waves. Besides, phase shifts deduced from integration under the curve for Rayleigh’s solitary waves are in better agreement with Byatt-Smith’s predictions than for KdV’s solitary waves. We suggest this is due to the better description in Rayleigh’s solution of the phase speed and outskirts decay coefficient. Another feature is that particles displacements at the free surface deduced from Rayleigh solution are very accurate. We thus derived a new analytical formula (31) for the limiting case of high-frequency short waves riding on large amplitude solitary waves. Experimentally, strong interactions have been carried out for the first time. They clearly show the influence on the phase shift determination of the direction of propagation of the waves interacting as far as small wave number are concerned. Besides, the only case, when taking into account experimental error, measurements enable to show a better agreement with one of the theoretical formulas, occurs in strong interaction. Thus, we show in that case that $\Delta\varphi_R$ and $\Delta\varphi_{\text{BS}}$ were in better agreement than $\Delta\varphi_{\text{KdV}}$ with measurements. In addition, we show that when the short wave wave number increases, phase shifts tends to the heuristic formula $\Delta\varphi_H$. Indeed, in our experimental set, we covered a broader range of short wave wave number than Clamond and Barthélemy.¹¹

During the experiments, some cases of breaking were observed that may be attributed to significant steepening of the short wave induced by both wave number and amplitude modulations. Indeed, breaking enables a difference to be made between two short wave trains with the same frequency but different amplitudes, whereas phase shift depends only on the frequency of the short wave. This latter appears

in the theory and is confirmed by the experiments. Relying on theoretical predictions, the maximum steepness reached at the crest of the solitary wave can be estimated using Byatt-Smith's numerical solution. It then appears that for similar maximum steepness predictions, short waves might be breaking in the strong interaction case whereas they do not in the weak interaction case, showing the influence of the underlying velocity.

ACKNOWLEDGMENTS

The authors would like to thank Jean-Marc Barnoud for technical support and assistance when performing the experiments. This work has been financially supported by the MAST-III EC Program, under Contract No. MAS3-CT95-0027.

- ¹M. S. Longuet-Higgins and R. W. Stewart, "Changes in form of short gravity waves on long waves and tidal currents," *J. Fluid Mech.* **8**, 565 (1960).
- ²M. S. Longuet-Higgins and R. W. Stewart, "The changes in amplitude of short gravity waves on steady non-uniform currents," *J. Fluid Mech.* **10**, 526 (1961).
- ³C. J. R. Garrett, "Discussion: the adiabatic invariant for wave propagation in a non-uniform moving medium," *Proc. R. Soc. London, Ser. A* **299**, 26 (1967).
- ⁴F. P. Bretherton and C. J. R. Garrett, "Wave trains in inhomogeneous moving media," *Proc. R. Soc. London, Ser. A* **302**, 529 (1969).
- ⁵M. S. Longuet-Higgins, "The propagation of short-surface waves on longer gravity waves," *J. Fluid Mech.* **177**, 293 (1987).
- ⁶M. Naciri and C. C. Mei, "Evolution of a short surface wave on a very long surface wave of finite amplitude," *J. Fluid Mech.* **235**, 415 (1992).
- ⁷J. Zhang and W. K. Melville, "Evolution of weakly non-linear short waves riding on long gravity waves," *J. Fluid Mech.* **214**, 321 (1990).
- ⁸I.-F. Shen, W. J. Easson, C. A. Greated, and W. A. B. Evans, "The modulation of short waves riding on solitary waves," *Phys. Fluids* **6**, 3317 (1994).
- ⁹W. A. B. Evans and M. J. Ford, "An exact integral equation for solitary waves (with new numerical results for some 'internal' properties)," *Proc. R. Soc. London, Ser. A* **452**, 373 (1996).
- ¹⁰D. Clamond and J.-P. Germain, "Interaction between a Stokes wave packet and a solitary wave," *Eur. J. Mech. B/Fluids* **18**, 67 (1999).
- ¹¹D. Clamond and E. Barthélemy, "Etude expérimentale du déphasage dans l'interaction houle-onde solitaire," *C. R. Acad. Sci. Paris. (IIB)* **320**, 277 (1995).
- ¹²J. W. Miles, "Obliquely interacting solitary waves," *J. Fluid Mech.* **79**, 157 (1977).
- ¹³M. S. Longuet-Higgins and O. M. Phillips, "Phase velocity effects in tertiary wave interactions," *J. Fluid Mech.* **12**, 333 (1962).
- ¹⁴Lord Rayleigh, "On waves," *Philos. Mag.* **1**, 257 (1876).
- ¹⁵D. J. Korteweg and G. De Vries, "On the change of form of long waves advancing in a rectangular canal, and on a new type of stationary waves," *Philos. Mag.* **39**, 422 (1895).
- ¹⁶J. G. B. Byatt-Smith, "An exact integral equation for steady surface waves," *Proc. R. Soc. London, Ser. A* **315**, 405 (1970).
- ¹⁷M. A. Lavrentiev, "On the theory of long waves," *Translation A.M.S.* **11**, 273 (1962).
- ¹⁸J. H. Shyu and O. M. Phillips, "The blockage of gravity and capillary waves by long waves and currents," *J. Fluid Mech.* **217**, 115 (1990).
- ¹⁹M. W. Dingemans, "Water waves propagation over uneven bottom, Part 1-Linear wave propagation," *Advanced Series on Ocean Engineering* (World Scientific, Singapore, 1997), Vol. 13.
- ²⁰C. C. Mei, "The applied dynamics of ocean surface waves," *Advanced Series on Ocean Engineering* (World Scientific, Singapore, 1992).
- ²¹J. G. B. Byatt-Smith and M. S. Longuet-Higgins, "On the speed and profile of steep solitary waves," *Proc. R. Soc. London, Ser. A* **350**, 175 (1976).
- ²²H. Lamb, *Hydrodynamics*, 6th ed. (Cambridge University Press, Cambridge, 1932), p. 738.
- ²³F. Serre, "Contribution à l'étude des écoulements permanents et variables dans les canaux," *La Houille Blanche* **8**, 374 (1953).
- ²⁴C. H. Su and C. S. Gardner, "KdV equation and generalizations. Part III. Derivation of Korteweg-de Vries equation and Burgers equation," *J. Math. Phys.* **10**, 536 (1969).
- ²⁵M. S. Longuet-Higgins, "Trajectories of particles at the surface of steep solitary waves," *J. Fluid Mech.* **110**, 239 (1981).
- ²⁶J. D. Fenton, "A ninth order solution for the solitary wave," *J. Fluid Mech.* **53**, 257 (1972).
- ²⁷M. S. Longuet-Higgins, "The trajectories of particles in steep, symmetrical gravity waves," *J. Fluid Mech.* **94**, 497 (1979).
- ²⁸F. Welt, "Plunger-type wave makers for high frequency waves," in *Rozprawy Hydrotechniczne* (Polska Akademia Nauk-Institut Budownictwa Wodnego, 1990), pp. 139-146.
- ²⁹W. G. Van Dorn, "Boundary dissipation of oscillatory waves," *J. Fluid Mech.* **24**, 769 (1966).
- ³⁰K. Guizien, "Les ondes longues internes: génération et interaction avec la houle," Thèse de l'Université Joseph Fourier, Grenoble, 1998.